Pharmacology, Biochemistry and Behavior 99 (2011) 428–436

Contents lists available at ScienceDirect

Pharmacology, Biochemistry and Behavior

journal homepage: www.elsevier.com/locate/pharmbiochembeh

Ethanol-induced changes in the expression of proteins related to neurotransmission and metabolism in different regions of the rat brain

Natalie M. Zahr [a,b,*], Richard L. Bell [c], Heather N. Ringham [d], Edith V. Sullivan [a], Frank A. Witzmann [d], Adolf Pfefferbaum [a,b]

[a] Psychiatry & Behavioral Sciences, Stanford University School of Medicine, 401 Quarry Rd., Stanford, CA 94305, USA
[b] Neuroscience Program, SRI International, 333 Ravenswood Rd., Menlo Park, CA, USA
[c] Department of Psychiatry, Indiana University School of Medicine, Institute of Psychiatric Research, 791 Union Drive, Indianapolis, IN 46202, USA
[d] Department of Cellular & Integrative Physiology, Indiana University School of Medicine, Biotechnology Research & Training Center, 1345 West 16th Street, Room 308, Indianapolis, IN 46202, USA

ARTICLE INFO

Article history:
Received 4 November 2010
Received in revised form 1 March 2011
Accepted 4 March 2011
Available online 11 March 2011

Keywords:
Vapor chambers
Proteomics
Frontocerebellar circuitry

ABSTRACT

Despite extensive description of the damaging effects of chronic alcohol exposure on brain structure, mechanistic explanations for the observed changes are just emerging. To investigate regional brain changes in protein expression levels following chronic ethanol treatment, one rat per sibling pair of male Wistar rats was exposed to intermittent (14 h/day) vaporized ethanol, the other to air for 26 weeks. At the end of 24 weeks of vapor exposure, the ethanol group had blood ethanol levels averaging 450 mg%, had not experienced a protracted (>16 h) withdrawal from ethanol, and revealed only mild evidence of hepatic steatosis. Extracted brains were micro-dissected to isolate the prefrontal cortex (PFC), dorsal striatum (STR), corpus callosum genu (CCg), CC body (CCb), anterior vermis (AV), and anterior dorsal lateral cerebellum (ADLC) for protein analysis with two-dimensional gel electrophoresis. Expression levels for 54 protein spots were significantly different between the ethanol- and air-treated groups. Of these 54 proteins, tandem mass spectroscopy successfully identified 39 unique proteins, the levels of which were modified by ethanol treatment: 13 in the PFC, 7 in the STR, 2 in the CCg, 7 in the CCb, 7 in the AV, and 5 in the ADLC. The functions of the proteins altered by chronic ethanol exposure were predominately associated with neurotransmitter systems in the PFC and cell metabolism in the STR. Stress response proteins were elevated only in the PFC, AV, and ADLC perhaps supporting a role for frontocerebellar circuitry disruption in alcoholism. Of the remaining proteins, some had functions associated with cytoskeletal physiology (e.g., in the CCb) and others with transcription/translation (e.g., in the ADLC). Considered collectively, all but 4 of the 39 proteins identified in the present study have been previously identified in ethanol gene- and/or protein-expression studies lending support for their role in ethanol-related brain alterations.

1. Introduction

Decades of postmortem and in vivo study have provided an extensive description of the untoward effects of chronic alcoholic exposure on brain morphology (cf., Chanraud et al., 2010; Pfefferbaum et al., 2004; Sullivan et al., 2010), neurochemistry (e.g., Durazzo et al., 2010), cellular structure (e.g., Pentney and Dlugos, 2000), and metabolism (e.g., Volkow et al., 1990) even in the absence of common concomitants of alcohol abuse such as thiamine deficiency (Butterworth, 1995) or liver disease (Anand, 1999). The mechanisms of disruption, however, are still not well understood. High-throughput assays, such as proteomics, are particularly useful in the investigation of complex, multi-factorial diseases like alcoholism, and provide a new avenue of exploration regarding the means whereby alcohol impairs the brain. Animal models, by providing control over the pattern of ethanol exposure, including age at initial exposure, dosage, and number of withdrawals, allow for specific inquiry uncompromised by variables that can rarely be controlled in the heterogeneous population of human alcoholics.

Ethanol-vapor exposure of rats is a method that results in rapid induction of dependence (Roberts et al., 2000). In the present study, the longitudinal effects of vaporized ethanol exposure were investigated in sibling pairs of wild-type Wistar rats, with one rat per pair exposed to escalating doses of vaporized ethanol, the other to vapor chamber air. In vivo magnetic resonance imaging (MRI) was used to evaluate brain structure and MR spectroscopy (MRS) to evaluate brain biochemistry before and twice during ethanol exposure. After 16 weeks, blood alcohol levels (BALs) approximated 300 mg% and after an additional 8 weeks (i.e., after 24 weeks), BALs approached 450 mg%. MRI revealed a profile of significant ventricular expansion

* Corresponding author at: Psychiatry & Behavioral Sciences, Stanford University School of Medicine, 401 Quarry Rd., Stanford, CA 94305, USA. Tel.: +1 650 859 5243; fax: +1 650 859 2743.
E-mail address: nzahr@stanford.edu (N.M. Zahr).

0091-3057/$ – see front matter © 2011 Elsevier Inc. All rights reserved.
doi:10.1016/j.pbb.2011.03.002

after ethanol vapor exposure: ventricular volume expanded by 8% in the controls, but by nearly 30% in the ethanol-exposed rats between baseline and week 24 (Pfefferbaum et al., 2008). Although enlargement of the lateral ventricles is assumed to result from atrophy of surrounding brain tissue, recent findings suggest that rather than overt cell loss, ventricular expansion likely reflects shrinkage of brain cells (including neurons, astrocytes, oligodendrocytes, and microglia) and their processes (Zahr et al., 2010b). MRS in a 0.25 cm^3 voxel containing the striatum revealed a significantly higher MRS-detectable signal from choline-containing compounds (Cho) at weeks 16 and 24 (Zahr et al., 2009). Higher levels of Cho can have various interpretations, including but not limited to inflammation, demyelination (Mader et al., 2008), impaired energy utilization (Djuricic et al., 1991), or cell membrane disruption (Griffin et al., 2001). Higher glutamine (Gln) was detected at week 16 (but not week 24), and higher glutamate (Glu) was observed at week 24 in the ethanol compared with the control group (Zahr et al., 2010a) indicating a disruption in Glu homeostasis.

To approach a mechanistic explanation for the changes observed in vivo, brains from these rats exposed to a total of 26 weeks of vaporized ethanol and their controls that had already undergone MR analysis were harvested and submitted to proteomic investigation. Several regions were selected because of their variable involvement in or susceptibility to ethanol-induced brain alterations (Harper, 2009). The basal ganglia, a key structure of which is the dorsal striatum (STR), was chosen because of its putative involvement in the loss of control over alcohol consumption (Tabakoff, 1979). The other brain regions were chosen either because of their known susceptibility to nutritional (i.e., thiamine) deficiencies (e.g., prefrontal cortex {PFC}, corpus callosum genu {CCg}, anterior vermis {AV}, and anterior dorsal lateral cerebellum {ADLC}) or because of their vulnerability to alcohol-related liver disease (e.g., AV and corpus callosum body {CCb}) (Matsumoto, 2009).

2. Methods

2.1. Study group

The initial study group comprised 10 sibling pairs of healthy male heterogeneous stock Wistar rats (Charles River Laboratories) that were singly housed with free access to food and water and acclimated to a reversed 14 h light/10 h dark cycle (i.e., lights on at 1900 to 0900 h for the rats' sleep cycle). The Institutional Animal Care and Use Committees at SRI International and Stanford University approved all procedures. This group of rats also underwent brain structural (with MRI Pfefferbaum et al., 2008) and biochemical (with MRS Zahr et al., 2009) examination.

2.2. Ethanol exposure

One rat from each sibling pair was exposed to a compressed mixture of ethanol and room air (ethanol group weight at the start of experiment: 625.88 ± 97.41 g) and the other to room air alone (control group weight: 629 ± 76.88 g) using a rodent ethanol inhalation system (La Jolla Alcohol Research Inc., La Jolla, CA) for a total of 26 weeks. In the first 16 weeks of ethanol exposure, 2 rats in the ethanol group died; an additional rat from the ethanol group died after the last MR examination before his brain could be properly harvested for proteomic analysis. Ethanol vapor was created by dripping 95% ethanol into a 4 L Erlenmeyer vacuum flask kept at 50 °C on a warming tray. Air was blown across the flask at 11 L/min to vaporize the ethanol. Concentrations of ethanol vapor were adjusted by varying the rate at which ethanol was pumped into the flask and ranged from 15 to 30 mg/L. Chambers administering intermittent vapor were connected to a timer that would turn the pumps on and off every day so that animals received ethanol vapor for 14 h at night during their sleep cycle (i.e., starting at 1900 h). Ethanol vapor exposure is a reliable technique allowing animals to move about freely and permitting maintenance of high and specific BALs (Roberts et al., 2000). Tail blood (~0.5 ml) sampled for BAL determination was collected into heparinized Eppendorf tubes. After centrifugation, the plasma was extracted and assayed for ethanol content based on direct reaction with the enzyme ethanol oxidase (Analox Instruments Ltd., London, UK). After 24 weeks of ethanol exposure, BALs in the ethanol group reached an average of 450 mg%. Rats did not experience protracted (>16 h) withdrawal at any time.

2.3. Neurological examination

To characterize behavior following prolonged (i.e., 24 weeks) ethanol exposure, each rat was evaluated with examination of 33 neurological signs (extracted from Becker, 2000; Pitkin and Savage, 2001) 1 h and 9 h after the pumps were turned off: two time points were chosen to test for potential differences in behavior between immediate exposure to and acute withdrawal from ethanol. After 24 weeks of exposure, the final MRI and MRS data were acquired. On the day prior to MR examination, within 1 h of ethanol exposure, all 8 alcoholized rats demonstrated neurological signs including lacrimation, nasal discharge, exophthalmoses, agitation, aggressiveness, and impairment of righting reflex. At 9 h after ethanol exposure, all 8 alcoholized rats continued to demonstrate altered autonomic and motor functions, and 4 of the 8 exhibited tremors (Zahr et al., 2009). The presence of tremor likely indicates acute withdrawal (Becker, 2000). Following the final MRI and MRS, all animals were placed back in their vapor chambers for 2 weeks until euthanasia.

2.4. Sample preparation and protein separation

After 26 weeks of ethanol exposure, within 3 h of being removed from their vapor chambers, animals were euthanized and their brains were extracted, flash-frozen, and stored at −80 °C. Subsequently, the PFC, STR, CCg, CCb, AV, and ADLC were micropunched for two-dimensional gel electrophoresis (2-DE, Fig. 1). For 2-DE, samples included appropriately preserved tissue from 6 ethanol-exposed animals and 7 control animals. Each brain tissue region consisted of 10 micropunched tissue samples except for the CCb, which consisted of 28 micropunched tissue samples. The samples were solubilized in 550 µL (1.1 mL for CCb) of a solubilization buffer containing 9 M urea, 4% CHAPS, 1% dithiothreitol (DTT), and 1% carrier ampholytes (pH 3–10). Samples were vortexed every 15 min for 1 h and incubated at 37 °C between vortex sessions. While it is well known that urea + heat + protein = carbamylation due to the formation of isocyanic acid and its reaction with the N-terminus, arginine, lysine, and cysteine residues of

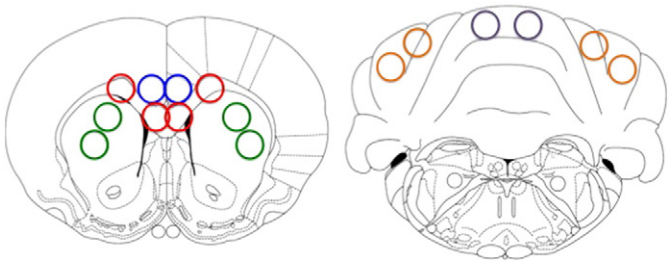

Fig. 1. Demonstrates the location and size of micropunches from the 6 regions evaluated. Ten punches were taken from the PFC (blue) in the ventral medial cortical structures anterior to the corpus callosum, 10 punches from the most anterior and dorsal portions of the STR (green), 38punches for CC genu and body (red) starting far anterior and ending at the hippocampus, 10 punches in the most anterior superior portions of the AV (purple), and 10 punches for the ADLC (orange), starting slightly posterior and lateral to the AV.

proteins, we have consistently shown that the brief incubation at 37 °C in the urea-based lysis buffers described above has no artifactual carbamylation effect on protein charge modification (Witzmann, 2005). After vortexing, each sample was sonicated using 3 × 2 s bursts at setting 3 with a Fisher Sonic Dismembrator every 15 min for 1 h and incubated at 37 °C between sonications. Protein concentration was determined using the 2-D Quant Kit (GE Healthcare, Pittsburgh, PA), an approach that enables the sensitive and accurate assay of solubilized proteins to be performed without interference from constituents of the lysis buffer.

2.5. Two-dimensional gel electrophoresis and image analysis

Using overnight, passive rehydration at room temperature, 200 μg of protein was loaded onto IPG strips (24 cm, nonlinear pH 3–10, BioRad, Hercules, CA). Isoelectric focusing (IEF) was performed simultaneously on all IPG strips randomly assigned to two Protean

Table 1
Identified Proteins (fold change numbers in bold reflect proteins significantly different between ethanol and air treated groups).

				Fold change					
	Identified protein	**P-value**	**Q-value**	**STR**	**PFC**	**CCg**	**CCb**	**AV**	**ADLC**
STR	Akr1c6	0.00001	0.312	**-1.4**	1.0	-1.2	-1.2	1.0	-1.3
	Idh3b	0.0019	0.435	**1.3**	1.0	1.0	1.0	1.0	-1.3
	Crym	0.0119	0.435	**-1.3**	-1.2	-1.1	-1.1	-1.2	-1.2
	Uchl1	0.0027	0.435	**-1.2**	1.0	1.0	1.0	1.0	1.2
	Aip	0.0122	0.435	**-1.2**	-1.1	1.0	1.0	1.1	1.1
	Stmn1	0.0056	0.435	**-1.2**	1.1	-1.1	-1.1	1.0	-1.1
	Ldhb	0.0122	0.435	**-1.1**	1.0	-1.1	-1.1	1.1	1.0
PFC	Tpm2	0.0105	0.414	1.1	**1.6**	1.4	1.3	1.0	1.2
	Gsto	0.0090	0.414	1.2	**1.4**	1.0	1.0	1.0	-1.3
	Mycl2b	0.0026	0.414	1.0	**1.3**	1.0	-1.1	1.0	1.0
	Syn2	0.0048	0.414	1.1	**1.2**	1.1	1.0	1.0	1.2
	Tkt	0.0138	0.414	1.1	**-1.2**	1.0	-1.1	1.1	1.1
	Hibch	0.0066	0.414	-1.2	**-1.2**	1.1	-1.2	1.1	1.1
	Cacybp	0.0068	0.414	1.0	**-1.2**	-1.1	1.0	-1.1	-1.1
	Itpa	0.0040	0.414	1.0	**1.2**	1.0	-1.1	1.1	-1.1
	Cox6a1	0.0088	0.414	1.0	**1.2**	1.0	1.0	1.1	1.0
	Gnb2l1	0.0050	0.414	-1.1	**-1.2**	-1.1	-1.2	1.0	-1.1
	Hspd1	0.0025	0.414	1.3	**1.2**	1.1	1.0	1.1	1.1
	Qdpr	0.0011	0.414	1.0	**-1.1**	1.0	1.0	-1.1	1.0
	Vdac2	0.0123	0.414	1.0	**-1.1**	1.1	1.0	1.0	1.1
CCg	Adk	0.0143	0.519	-1.1	1.0	**-1.2**	-1.2	1.0	1.0
	Pkm2	0.0141	0.519	-1.1	1.0	**-1.2**	-1.2	-1.1	1.1
CCb	Eif5a	0.0030	0.447	1.0	1.0	1.0	**-1.4**	1.0	-1.1
	Tuba1α	0.0010	0.447	1.0	1.0	1.0	**-1.3**	-1.1	-1.1
	Fabp7	0.0098	0.447	-1.2	-1.1	-1.1	**-1.2**	1.0	-1.1
	Pdia3	0.0133	0.447	-1.2	1.0	-1.1	**-1.2**	1.0	1.1
	Tuba1α	0.0088	0.447	1.0	1.1	1.0	**-1.2**	1.0	-1.1
	Arhgdia	0.0072	0.447	1.0	1.0	-1.1	**-1.2**	1.1	1.0
	Nefl	0.0143	0.447	1.0	1.1	1.1	**1.2**	-1.3	1.1
AV	Hbb	0.0151	0.507	1.0	1.2	1.0	-1.1	**-1.4**	-1.1
	Snap25	0.0147	0.507	1.0	1.0	-1.1	-1.1	**-1.3**	-1.3
	Snap25	0.0095	0.507	1.0	1.0	-1.2	-1.1	**-1.2**	-1.2
	Hspa5	0.0022	0.507	1.3	1.0	1.1	1.3	**1.2**	1.2
	Tufm	0.0047	0.507	1.0	1.0	1.1	1.2	**1.2**	1.1
	Hsd17b10	0.0022	0.507	1.1	1.0	1.2	1.0	**1.2**	1.0
	Actb	0.0118	0.507	1.0	1.0	1.0	1.0	**1.1**	1.0
ADLC	Acta1	0.0141	0.394	-1.1	-1.1	-1.2	-1.2	-1.1	**-1.3**
	Prdx5	0.0130	0.394	1.0	1.0	1.2	1.0	1.0	**1.3**
	Hist1h4b	0.0131	0.394	1.3	1.2	1.0	-1.3	1.0	**-1.3**
	Nme1	0.0105	0.394	1.0	1.1	1.1	1.0	1.0	**1.3**
	Phox2a	0.0142	0.394	1.0	1.0	1.0	1.3	1.0	**1.2**

IEF Cells (BioRad, 10 strips/instrument) by a program of progressively increasing voltage (150 V for 2 h, 300 V for 4 h, 1500 V for 1 h, 5000 V for 5 h, 7000 V for 6 h, and 10,000 V for 3 h) for a total of 100,000 V h.

First-dimension IPG strips were loaded directly onto second-dimension sodium dodecyl sulfate (SDS) slab gels (20×25×0.15 cm) with a 10–20% acrylamide gradient (Jule, Inc.) following equilibration for 10 min in Equilibration Buffer I (6 M urea, 2% SDS, 0.375 M Tris–HCl pH 8.8, 20% glycerol, 130 mM DTT) and 10 min in Equilibration Buffer II (6 M urea, 2% SDS, 0.375 M Tris–HCl pH 8.8, 20% glycerol, 135 mM iodoacetamide). All 13 second-dimension slab gels (7 control samples, 6 ethanol-treated samples {1 gel/sample} for each of the 6 regions equals a total of 78 gels) were run in parallel at 8 °C for 20 h at 160 V and subsequently fixed and stained using a modified colloidal Coomassie Blue G-250 procedure with 1 ng protein/spot sensitivity (Candiano et al., 2004). After 96 h, gels were washed several times with water and scanned at 95.3-μm/pixel resolution using an ImageScanner III (GE Healthcare, Pittsburgh, PA).

The resulting 12-bit images were analyzed using Progenesis SameSpots™ (v3.0, Nonlinear Dynamics, Durham, NC) and its embedded ANOVA analytic software. Alpha was set at $p \leq 0.015$ for all analyses. Six separate analyses were performed for each of the brain regions. Each analysis consisted of a one-way ANOVA comparing control vs. ethanol treated samples. Background was subtracted and protein spot density peaks were detected and counted. Because total spot counts and the total optical density are directly related to the total protein concentration (Maldve et al., 2002), individual protein quantities were expressed as parts per-million (ppm) of the total integrated optical density after normalization against total image density. A reference pattern was selected and each of the gel images in the match-set was matched to the reference pattern using the software's advanced automated image alignment. Raw quantitative data for each protein spot were then analyzed statistically.

2.6. Mass spectrometry

Protein spots of interest were manually excised from the gels. The protein spots were destained, reduced with DTT, alkylated with iodoacetamide, and tryptically digested using sequence grade, modified trypsin (Princeton Separations, Freehold, NJ). Resulting peptides were extracted from the gel plugs through a series of buffer exchanges, including 0.1% FA in 30% ACN, 0.1% FA in 50% ACN, and 100% ACN. Subsequently, peptides were concentrated and purified via speed vacuum centrifugation followed by a ZipTip® (Millipore, Billerica, MA) protocol.

Peptide samples (40 μL) were injected into a Thermo Scientific (Waltham, MA) LTQ linear ion trap mass spectrometer using a Michrom Paradigm AS1 auto-sampler coupled to a Paradigm MS4 High Performance Liquid Chromatography (HPLC) column (Michrom BioResources, Inc., Auburn, CA). The peptide solution was automatically loaded at a flow rate of 0.5 μL/min across a Paradigm Platinum Peptide Nanotrap (Michrom BioResources, Inc.) and onto a 150×0.099 mm capillary column (Polymicro Technologies, L.L.C., Phoenix, AZ) packed in-house using a 5 μm, 100 Å pore size Magic C18 AQ stationary phase (Michrom BioResources, Inc.). Mobile phases A (2% acetonitrile in 0.1% formic acid), B (98% acetonitrile in 0.1% formic acid), and C (5% acetonitrile in 0.1% formic acid) were all made in HPLC grade water. Buffer C was used to load the sample, and the gradient elution profile was as follows: 5% B (95% A) for 10 min; 5–55% B (95–45% A) for 30 min; 55–80% B (45–20% A) for 5 min; and 80–5% B (20–95% A) for 10 min. The data were collected in a "Triple-Play" (MS scan, Zoom scan, and MS/MS scan) mode using nanospray ionization with normalized collision energy of 35%.

The acquired mass spectral data were searched against the International Protein Index rat database (ipi.RAT.v337) using the SEQUEST (v. 28, rev. 12) program in Bioworks (v. 3.3, Thermo Scientific) (Curtin et al., 2009). General parameters were set as follows: peptide tolerance 2.0 atomic mass units (AMU), fragment ion tolerance 1.0 AMU, enzyme limits set as "fully enzymatic — cleaves at both ends" and missed cleavage sites set at 2. The searched peptides and proteins were subjected to the validation processes PeptideProphet (Keller et al., 2002) and ProteinProphet (Nesvizhskii and Aebersold, 2004) in the Trans-Proteomic Pipeline (v. 3.3.0) (http://tools.proteomecenter.org/software.php), and only those proteins with greater than 90% confidence were considered positive identifications. Protein functions were derived from either the EntrezGene or UnitProtKB/Swiss-Prot entries provided at GeneCards® (www.genecards.org).

3. Results

Approximately 2000 proteins were resolved, matched, and analyzed in 2-D gel patterns of the various brain regions studied. The expression levels of 54 protein spots were significantly different between the ethanol ($n=6$) and air ($n=7$) treated groups. Of the 54, tandem mass spectroscopy successfully identified 39 differentially expressed unique proteins and 2 post-translationally modified proteins (Tables 1 and 2). Of the 17 spots in the PFC, 13 were identified (6 down-regulated); 7 of 8 spots were identified in the STR (6 down-regulated), 2 of 5 spots were identified in the CCg (both down-regulated), 7 of 7 spots were identified in the CCb (6 down-regulated, 1 *isoform*), 7 of 9 spots were identified in the AV (3 down-regulated, 1 *isoform*), and 5 of 8 spots were identified in the ADLC (2 down-regulated). One of the proteins identified in the CCb (i.e., TUBA1A) and one in the AV (i.e., SNAP25) appeared in 2 separate spots suggesting post-translational-modification of the same protein. Comparison of the identified proteins in various brain region images by homologous position suggests that the majority of these proteins were present in all regions analyzed, but the statistically significant differences in expression levels were unique to the regions mentioned.

4. Discussion

Proteomic analysis using 2-DE and tandem mass spectrometry identified 39 unique proteins in 6 different brain regions, the levels of which were significantly modified by 26 weeks of vaporized ethanol exposure. The proteins changed with chronic ethanol exposure were selective to each brain region examined and could be distinguished by function (Table 3). Regional grouping by function highlights brain circuits relevant to alcohol use disorders. In particular, the levels of stress response proteins (i.e., Gsto, Hspd1, Hspa5, and Prdx5) were elevated only in the PFC and both regions of the cerebellum sampled (i.e., AV and ADLC), but in none of the other regions examined. This selective finding may support the hypothesized role of dysfunctional frontocerebellar circuitry in contributing to characteristic behaviors of alcoholics (e.g., Sullivan et al., 2003; Zahr et al., 2010). This concept is further supported by the finding that the PFC and the cerebellum may be particularly responsive to ethanol as evidenced by the higher number of proteins identified in these regions (13 in the PFC and 12 in the combined cerebellar regions) compared to the others.

The PFC also revealed nearly all of the neurotransmitter-related protein changes observed, including those related to both glutamate and dopamine signaling (i.e., Syn2, Gnb2l1, Vdac2, and Qdpr). This finding emphasizes the sensitivity of the PFC to alterations in neurotransmitter function and the potential neuroadaptations that occur in the PFC during addiction (Koob and Volkow, 2010). Indeed, the shift to habitual behavior (i.e., addiction) seems to depend, in part, on glutamatergic projections from the PFC to the ventral striatum (Kalivas and O'Brien, 2008).

Four of the nine proteins identified in the combined corpus callosal regions had metabolic functions. Both pathological (Harper and Kril, 1988; Tarnowska-Dziduszko et al., 1995) and structural MRI (Estruch et al., 1997; Pfefferbaum et al., 1996) studies demonstrate that the area of corpus callosum is reduced and its microstructure compromised (Pfefferbaum et al., 2006, 2009) in alcoholics. A metabolic compromise

Table 2
Alphabetic listing of identified proteins that were changed, their relative abundance as a percent of control levels, the brain region which displayed this significant ($P<0.05$) difference, and a general description of their function.

Gene ID	% of control	Protein ID	Description
Acta1	76% in ADLC	Actin α1	A cytoskeletal protein; major constituent of the contractile apparatus of skeletal muscle; missense mutations of the Acta1 gene reported to be associated with brain deformities and cognitive impairment (Goez et al., 2005).
Actb	107% in AV	Actin β	A cytoskeletal protein involved in cell motility, structure, and integrity.
Adk	86% in CCg	Adenosine kinase	Catalyzes the transfer of the γ-phosphate from ATP to adenosine, thereby regulating concentrations of both extracellular adenosine and intracellular adenine nucleotides.
Aip	82% in STR	Aryl-hydrocarbon receptor-interacting protein	A ligand-activated transcription factor/receptor for aryl hydrocarbons; it regulates the expression of xenobiotic metabolizing enzymes and inhibits the activity of cyclic AMP phosphodiesterase; it may regulate survivin stability (Kang and Altieri, 2006) implicating a role in combating apoptosis.
Akr1c6	73% in STR	Aldo-keto reductase family 1, member C6	Active toward androgens, estrogens, and xenobiotics catalyzing the conversion of aldehydes and ketones to their corresponding alcohols using NADH or NADPH as cofactors.
Arhgdia	86% in CCb	Rho GDP dissociation inhibitor (GDI) alpha	Aplysia Ras-related homologs, also called Rho genes may be kept in the inactive, guanosine diphosphate (GDP)-bound state by interaction with GDP dissociation inhibitors such as Arhgdia.
Cacybp	84% in PFC	Calcyclin binding protein	Involved in calcium-dependent ubiquitination and subsequent proteosomal degradation; frequently colocalized with tau and tubulin suggesting a role in cytoskeletal physiology (Filipek et al., 2008).
Cox6a1	117% in PFC	Cytochrome C oxidase polypeptide VIa-liver (mitochondrial precursor)	The terminal enzyme of the mitochondrial respiratory chain; catalyzes the electron transfer from reduced cytochrome C to oxygen; implicated in controlling apoptosis via BAK (Eun et al., 2008).
Crym	79% in STR	Mu-crystallin homolog	Possesses catalytic and deaminase activity; implicated in the regulation of intracellular concentrations of thyroid hormone.
Eif5a	73% in CCb	Eukaryotic translation initiation factor 5A-1	An mRNA-binding protein important for translation elongation and mRNA turnover; involved in actin dynamics, cell-cycle progression, stress responses, maintenance of cell-wall integrity (Chatterjee et al., 2006); can regulate apoptosis via interactions with p53 and TNF-α (Rahman-Roblick et al., 2007).
Fabp7	82% in CCb	Fatty acid binding protein, brain	Binds long-chain fatty acids and other hydrophobic ligands regulating their uptake, transport, and metabolism.
Gnb2l1	86% in PFC	G-protein, subunit β-2-like-1	Implicated in intracellular binding of protein kinase C; via its association with SRC may be involved in PI3K and MAPK signaling pathways involved in cell proliferation, migration, and survival (Cozzoli et al., 2009; Roberto et al., 2003).
Gsto	144% in PFC	Glutathione S-transferase Ω 1	Acts as a small stress response protein, a glutathione-dependent dehydroascorbate reductase, and is implicated in cellular redox homeostasis.
Hbb	73% in AV	Hemoglobin subunit β-1	The β-globin chain of hemoglobin, which binds and transports oxygen to tissue.
Hibch	82% in PFC	3-Hydroxyisobutyryl-coenzyme A hydrolase (isoform 2)	Participates in 3 metabolic pathways: valine, leucine and isoleucine degradation; beta-alanine metabolism; and propanoate metabolism.
Hist1h4b	78% in ADLC	Histone cluster 1, H4b (isoform)	Histones interact with linker DNA between nucleosomes and function in the compaction of chromatin into higher order structures and thereby play an important role in transcription regulation, DNA repair, DNA replication, and chromosomal stability.
Hsd17b10	116% in AV	17-β-Hydroxysteroid dehydrogenase 10	Also known as 3-hydroxyacyl-CoA dehydrogenase type II; a member of the short-chain dehydrogenase/reductase superfamily that catalyze the oxidation of a wide variety of fatty acids, alcohols, and steroids.
Hspa5	121% in AV	Heat shock protein 5 (glucose-regulated protein, 78 kDa)	A member of the chaperonin family of proteins whose expression increases under stress; prevents misfolding and promotes refolding and proper assembly of unfolded polypeptides generated under stress conditions;
Hspd1	115% in PFC	Heat shock protein 1 (mitochondrial, 10 kDa)	A member of the chaperonin family of proteins whose expression increases under stress; prevents misfolding and promotes refolding and proper assembly of unfolded polypeptides generated under stress conditions; may also function as a signaling molecule in the cellular immune response.
Idh3b	127% in STR	Isocitrate dehydrogenase [NAD+] subunit β	Catalyzes the oxidative decarboxylation of isocitrate to 2-oxoglutarate
Itpa	118% in PFC	Inosine triphosphatase	A metabolic protein that hydrolyzes inosine triphosphate and deoxyinosine triphosphate to the monophosphate and diphosphate nucleotides.
Ldhb	91% in STR	L-lactate dehydrogenase B chain	Functions in the glycolytic pathway catalyzing the interconversion of lactate and pyruvate; implicated in the expression of cell surface antigens during T cell development (Fujishiro et al., 2000).
Mylc2b	128% in PFC	Myosin regulatory light chain 2-B (smooth muscle isoform)	A cytoskeletal protein implicated in cell locomotion and cytokinesis.
Nefl	116% in CCb	Neurofilament light polypeptide	A constituent of the axoskeleton; helps functionally maintain neuronal caliber; implicated in intracellular transport to axons and dendrites.
Nme1	126% in ADLC	Nucleoside diphosphate kinase A	Implicated in the synthesis of nucleoside triphosphates other than ATP; involved in cell proliferation, differentiation, and development, signal transduction, G protein-coupled receptor endocytosis, and gene expression.
Pdia3	83% in CCb	Protein disulfide isomerase A3 precursor	Interacts with calreticulin and calnexin to modulate folding of newly synthesized glycoproteins; plays a cytoprotective role against oxidative stress; functions in antigen presentation and T cell responses (Garbi et al., 2006).
Phox2a	122% in ADLC	Paired homeobox protein 2A	A transcription factor that regulates the expression of tyrosine hydroxylase and dopamine beta-hydroxylase, two catecholaminergic biosynthetic enzymes essential for the differentiation and maintenance of the central noradrenergic system.
Pkm2	84% in CCg	Pyruvate kinase isozymes M1/M2 (isoform M1)	A glycolytic enzyme that catalyzes the transfer of a phosphoryl group from phosphoenolpyruvate to ADP generating pyruvate and ATP; interacts with thyroid hormone mediating its metabolic effects (Sabell et al., 1985).
Prdx5	128% in ADLC	Peroxiredoxin 5 (isoform)	An antioxidant enzyme that reduces hydrogen peroxide and alkyl hydroperoxides

Table 2 (*continued*)

Gene ID	% of control	Protein ID	Description
			and thus implicated in antioxidant neuroprotection.
Qdpr	87% in PFC	Dihydropteridine reductase	Catalyzes the NADH-mediated reduction of quinonoid dihydrobiopterin to tetrahydrobiopterin, which is an essential cofactor for phenylalanine, tyrosine, and tryptophan hydroxylases, enzymes necessary for the production of the neurotransmitters dopamine and serotonin.
Snap25	77% in AV	Synaptosomal-associated protein, 25 kDa, isoform 25b (charge variant)	A presynaptic plasma membrane protein associated with scaffolding proteins involved in vesicle docking and membrane fusion, thus regulating neurotransmitter release; implicated in axonal growth.
Snap25	80% in AV	Synaptosomal-associated protein, 25 kDa, isoform 25b (charge variant)	A presynaptic plasma membrane protein associated with scaffolding proteins involved in vesicle docking and membrane fusion, thus regulating neurotransmitter release; implicated in axonal growth.
Stmn1	83% in STR	Stathmin	A ubiquitous cytosolic phosphoprotein implicated in integrating regulatory signals of the cellular environment; involved in regulating the microtubule filament system; STMN1 knock-out mice are deficient in innate and learned fear (Martel et al., 2008).
Syn2	123% in PFC	Synapsin 2 (isoform IIa)	A neuron-specific phosphoprotein involved in vesicle trafficking to synapses, the regulation of neurotransmitter release, and synaptic morphology.
Tkt	81% in PFC	Transketolase	Connects the pentose phosphate pathway to glycolysis, feeding excess sugar phosphates into the main carbohydrate metabolic pathway.
Tpm2	156% in PFC	Tropomyosin β chain (isoform 2)	A cytoskeletal protein that regulates actin binding and ATPase activity.
Tuba1α	77% in CCb	Tubulin α 1A chain (charge variant)	A cytoskeletal protein that forms heterodimers with β-tubulin; acts as a structural component of the microtubule cytoskeleton; plays a role in microtubule-based processes; colocalized with Cacybp.
Tuba1α	83% in CCb	Tubulin α 1A chain (charge variant)	A cytoskeletal protein that forms heterodimers with ß-tubulin; acts as a structural component of the microtubule cytoskeleton; plays a role in microtubule-based processes; colocalized with Cacybp.
Tufm	118% in AV	Tu translation elongation factor	Participates in protein translation/synthesis.
Uchl1	80% in STR	Ubiquitin carboxyl-terminal hydrolase isozyme L1	Involved in the processing of ubiquitinated proteins; implicated in axonogenesis (Saigoh et al., 1999).
Vdac2	91% in PFC	Voltage-dependent anion-selective channel 2	Implicated in Ca2+ homeostasis and ATP production/availability; interacts with the GABA-A benzodiazepine complex (Mehta and Ticku, 1999); can bind neurosteroids, and implicated in controlling apoptosis via BAK (Cheng et al., 2003).

ADLC = Anterior Dorsal Lateral Cerebellum; AV = Anterior Vermis; CCB = Corpus Callosum Body; CCG = Corpus Callosum Genu; STR = Dorsal Striatum; PFC = Prefrontal Cortex.

may explain the reduction of the corpus callosum area often seen in alcoholics.

All but one of the seven proteins changed in the STR had functions related to metabolism. Altogether, 16 of the 41 proteins identified in this study had functions related to metabolism including the regulation of fundamental cellular processes (e.g., Stmn1 and Uchl1) and the normal production of ATP (e.g., Adk, Cox6a1, Ldhb, and Pkm2). The general decrease in the levels of these proteins might indicate a compromise to the normal functioning of brain cells. Indeed, these in vitro results may provide a potential mechanistic explanation for the in vivo MRI finding of ventricular enlargement (Pfefferbaum et al., 2008). If brain cells are metabolically compromised, an adaptive response may be the decrease or deletion of their dendritic arbor (e.g., Sullivan et al., 2003) resulting in the appearance of brain volume shrinkage (Zahr et al., 2010b).

Such protein changes may also provide an explanation for the increase in brain Cho observed using MRS following the 16 and 24 weeks of ethanol exposure. Potential interpretations for higher levels of Cho include cell membrane disruption (Griffin et al., 2001) or demyelination (Mader et al., 2008). At least 7 (i.e., Acta1, Actb, Cacybp,

Table 3
Listing of identified proteins by region and function. (Red- higher than controls; Blue lower than controls).

	Neurotransmission	Metabolism	Cytoskeleton	Stress response	Transcription/translation
PFC	Syn2 Gnb2l1 Vdac2 Qdpr	Cox6a1 Itpa Hibch Tkt	Mycl2b Tpm2 Cacybp	Gsto Hspd1	
STR		Idh3b Akr1c6 Crym Ldhb Stmn1 Uchl1			Aip
CCg		Adk Pkm2			
CCb	Arhgdia	Fabp7 Pdia3	Nefl Tuba1α		Eif5a
AV	Snap25	Hsd17b10 Hbb	Actb	Hspa5	Tufm
ADLC	Nme1		Acta1	Prdx5	Phox2a Hist1h4b

Mylc2b, Nefl, Tpm2, and Tuba1α) of the 39 uniquely identified proteins in this study are cytoskeletal. Adaptive changes to the structure of brain cells such as retraction of their dendritic arbor (i.e., cell membrane disruption) or demyelination (cf., He et al., 2007; Mayfield et al., 2002; Pfefferbaum et al., 2009) could result in an altered cytoskeleton and release of Cho-containing compounds (Zeisel, 1993).

Over 500 proteins have been identified as altered by ethanol in brain tissue collected from humans and rodents: frontal cortex (Alexander-Kaufman et al., 2007a, 2006; Etheridge et al., 2009; Lewohl et al., 2004), occipital cortex (Etheridge et al., 2009), hippocampus (Hargreaves et al., 2009; Matsuda-Matsumoto et al., 2007), corpus callosum (Kashem et al., 2008, 2007), nucleus accumbens (Bell et al., 2006; McBride et al., 2009; Witzmann et al., 2003), amygdala (Bell et al., 2006), and cerebellar vermis (Alexander-Kaufman et al., 2007b). Accordingly, as presented in Table 4, the majority of the proteins detected in the current study have previously been identified as altered by ethanol exposure in human and rodent, genomic or proteomic studies. In human studies, it is difficult to control for and report the number, frequency, or length of abstinence attempts or withdrawals. With respect to rodent experiments, one of the previous ethanol-related proteomics studies describes the results of either multiple scheduled access or continuous free-choice access to ethanol with brains harvested within 12 h of the last ethanol exposure (Bell et al., 2006). In another two of the ethanol-related proteomics studies in rats referenced herein (e.g., Masuo et al., 2009; McBride et al., 2009), 24 h of abstinence preceded euthanasia, and in a final study, 2 weeks of an alcohol-free "washout period" preceded tissue extraction (Hargreaves et al., 2009). Thus, in all but one of the rodent proteomics studies previously conducted in which ethanol exposure was manipulated, the findings are primarily due to the consequences of ethanol exposure and not of protracted withdrawal (i.e., the ethanol withdrawal period did not exceed 24 h).

Of the 39 unique proteins identified in the current study, only 4 have not been previously reported as altered by ethanol: Adk, Hibch, Itpa, and Phox2a. Despite their absence in the literature regarding gene or protein responsivity to ethanol, both Adk and Hibch may be associated with alcohol use disorders. Adenosine kinase (i.e., Adk) regulates the concentration of adenosine, an endogenous purine nucleoside that modulates many physiological processes. Ethanol inhibits adenosine reuptake and increases extracellular adenosine (Mailliard and Diamond, 2004). Similarly, in cirrhosis of the liver, a common complication of chronic alcoholism (Mann et al., 2003), Hibch activity in the liver is low (Ishigure et al., 2001; Taniguchi et al., 1996). To our knowledge, this is the first documentation of alterations in Itpa or Phox2a following ethanol exposure.

Although the false discovery rates (FDR, Q-values and associated p-values, Table 1) obtained herein suggest modest to high false positive levels, the fact that the majority of proteins identified in this study have been reported from both preclinical and post-mortem clinical studies supports replication of previous findings. While the observed replications with previous findings provide confidence in the results, the fact that different methodologies were used indicates caution is warranted when interpreting the present findings. To provide even greater support for similar findings in the future, especially when modest to high FDR are present, protein expression differences can be validated immunologically using Western blot analyses. Alternatively, if suitable antibodies are not available, validation can be done using mass spec-based selected reaction monitoring (SRM).

5. Conclusions

Brains of heterogeneous stock Wistar rats exposed to 26 weeks of vaporized ethanol differed from non-exposed controls in the expression levels of 41 proteins involved in selective cellular

Table 4
Alphabetic listing of gene ID's for identified proteins that were changed in the present study and previous reports implicating its, or an isoform's role in alcoholism.

Gene ID	Rodent studies	Human studies
Acta1	Δ gene expression5,19,27	Δ gene expression12
	Δ protein expression4,26,41	Δ protein expression2,3,9,16,21
Actb	Δ gene expression5,19,27	Δ gene expression12
	Δ protein expression4,26,41	Δ protein expression2,3,9,16,21
Adk		
Aip	Δ gene expression27	
	Δ protein expression23	
Akr1c6	Δ gene expression6	Δ gene expression15
Arhgdia		Δ gene expression12,38
Cacybp	Δ gene expression5	
Crym		Δ gene expression25
		Δ protein expression2,17
Cox6a1	Δ gene expression7,27,28,30,32	Δ gene expression33
	Δ protein expression26	
Eif5a	Δ gene expression13,28,30	Δ gene expression29
Fabp7	Δ gene expression39	Δ gene expression29
	Δ protein expression11	Δ protein expression21
Gnb2l1	Δ gene expression28,32,36,40	Δ gene expression20
	Δ protein expression26	
Gsto	Δ gene expression13,19,31	Δ gene expression15
	Δ protein expression26	Δ protein expression17
Hbb	Δ gene expression19	
Hibch		
Hist1h4b	Δ gene expression30	Δ gene expression15, 20
	Δ protein expression26	
Hsd17b10	Δ gene expression30	
Hspd1	Δ gene expression7	Δ gene expression20
	Δ protein expression4,26,41	Δ protein expression2,9,17,21
Hspa5	Δ gene expression7	Δ gene expression20
	Δ protein expression4,26,41	Δ protein expression2,9,17,21
Aldh3b	Δ gene expression32	Δ gene expression12
		Δ protein expression16,17
Itpa		
Ldhb	Δ gene expression35	
	Δ protein expression26,41	Δ protein expression3,9,17
Mylc2b		Δ gene expression33
Nefl	Δ gene expression27	Δ gene expression38
	Δ protein expression26	Δ protein expression2,16,17
Nme1	Δ gene expression5	Δ gene expression12
	Δ protein expression26	
Pdia3	Δ gene expression6	Δ gene expression33
		Δ protein expression3,17
Phox2a		
Pkm2		
	Δ protein expression26	Δ protein expression2,3,21
Prdx5	Δ gene expression27	
		Δ protein expression3,16,21
Qdpr	Δ gene expression8,19,37	
		Δ protein expression3
Snap25	Δ gene expression19	
	Δ protein expression4,26	Δ protein expression2,17
Stmn1	Δ gene expression34	
		Δ protein expression16
Syn2	Δ gene expression8,19,27	Δ gene expression25
	Δ protein expression11	
Tkt	Δ gene expression19,34	Δ gene expression22
		Δ protein expression1,2,3
Tpm2	Δ gene expression6,13,30,40	
	Δ protein expression4	Δ protein expression16,17,21
Tuba1a	Δ gene expression19,37,40	Δ gene expression10
	Δ protein expression26	Δ protein expression16,17,21
Tufm		
	Δ protein expression26	Δ protein expression2,3
Uchl1	Δ gene expression27,42	
	Δ protein expression11	Δ protein expression1,21,24
Vdac2		
	Δ protein expression4,26	Δ protein expression2,21

1 Alexander-Kaufman et al., 2006; 2 Alexander-Kaufman et al., 2007a; 3 Alexander-Kaufman et al., 2007b; 4 Bell et al., 2006; 5 Bell et al., 2009; 6 Carr et al., 2007; 7 Ciccocioppo et al., 2006; 8 Edenberg et al., 2005; 9 Etheridge et al., 2009; 10 Flatscher-Bader et al., 2005; 11 Hargreaves et al., 2009; 12 Hill et al., 2004; 13 Hitzemann et al., 2004; 14 Hoffman and Tabakoff, 2005; 15 Iwamoto et al., 2004; 16 Kashem et al., 2007; 17 Kashem et al., 2008; 18 Kerns et al., 2005; 19 Kimpel et al., 2007; 20 Lewohl et al., 2000; 21 Lewohl et al., 2004; 22 Liu et al., 2006; 23 Masuo et al., 2009; 24 Matsuda-Matsumoto et al., 2007; 25 Mayfield et al., 2002; 26 McBride et al., 2009; 27 McBride et al., 2010; 28 Mulligan et al., 2006; 29 Prescott et al., 2006; 30 Rodd et al., 2008; 31 Saba et al., 2006; 32 Saito et al., 2004; 33 Sokolov et al., 2003; 34 Sommer et al., 2006; 35 Tabakoff et al., 2003; 36 Tabakoff et al., 2008; 37 Tabakoff et al., 2009; 38 Thibault et al., 2000; 39 Treadwell and Singh, 2004; 40 Wang et al., 2007; 41 Witzmann et al., 2003; 42 Xu et al., 2001.

processes. Processes implicated include neurotransmission, metabolism, cytoskeletal physiology, stress responses, and transcription/translation. Based on the high number of responsive genes in the PFC and cerebellum and the commonality of their functions, the findings here may support the hypothesized role of frontocerebellar dysfunction in alcoholism. In addition, the high number of metabolic proteins with ethanol-associated altered expression levels may provide a potential mechanism for the ventricular expansion and callosal shrinkage commonly observed in chronic alcoholics.

Acknowledgments

The National Institute on Alcohol Abuse and Alcoholism provided support for this research with grants to AP (AA005965, AA013521-INIA), EVS (AA017168), and RLB (AA013522-INIA).

Appendix A. Supplementary data

Supplementary data to this article can be found online at doi: doi:10.1016/j.pbb.2011.03.002.

References

Alexander-Kaufman K, Dedova I, Harper C, Matsumoto I. Proteome analysis of the dorsolateral prefrontal region from healthy individuals. Neurochem Int 2007a;51: 433–9.
Alexander-Kaufman K, Harper C, Wilce P, Matsumoto I. Cerebellar vermis proteome of chronic alcoholic individuals. Alcohol Clin Exp Res 2007b;31:1286–96.
Alexander-Kaufman K, James G, Sheedy D, Harper C, Matsumoto I. Differential protein expression in the prefrontal white matter of human alcoholics: a proteomics study. Mol Psychiatry 2006;11:56–65.
Anand BS. Cirrhosis of liver. West J Med 1999;171:110–5.
Becker HC. Animal models of alcohol withdrawal. Alcohol Res Health 2000;24:105–13.
Bell RL, Kimpel MW, Rodd ZA, Strother WN, Bai F, Peper CL, et al. Protein expression changes in the nucleus accumbens and amygdala of inbred alcohol-preferring rats given either continuous or scheduled access to ethanol. Alcohol 2006;40:3–17.
Bell RL, Kimpel MW, McClintick JN, Strother WN, Carr LG, Liang T, Rodd ZA, Mayfield RD, Edenberg HJ, McBride WJ. Gene expression changes in the nucleus accumbens of alcohol-preferring rats following chronic ethanol consumption. Pharmacol Biochem Behav 2009;94:131–47.
Butterworth RF. Pathophysiology of alcoholic brain damage: synergistic effects of ethanol, thiamine deficiency and alcoholic liver disease. Metab Brain Dis 1995;10: 1–8.
Candiano G, Bruschi M, Musante L, Santucci L, Ghiggeri GM, Carnemolla B, et al. Blue silver: a very sensitive colloidal Coomassie G-250 staining for proteome analysis. Electrophoresis 2004;25:1327–33.
Carr LG, Kimpel MW, Liang T, McClintick JN, McCall K, Morse M, Edenberg HJ. Identification of candidate genes for alcohol preference by expression profiling of congenic rat strains. Alcohol Clin Exp Res 2007;31:1089–98.
Chanraud S, Pitel AL, Sullivan EV. Structural imaging of alcohol abuse. In: Shenton ME, Turetsky BI, editors. Understanding neuropsychiatric disorders. Cambridge University Press; 2010.
Chatterjee I, Gross SR, Kinzy TG, Chen KY. Rapid depletion of mutant eukaryotic initiation factor 5A at restrictive temperature reveals connections to actin cytoskeleton and cell cycle progression. Mol Genet Genomics 2006;275:264–76.
Cheng EH, Sheiko TV, Fisher JK, Craigen WJ, Korsmeyer SJ. VDAC2 inhibits BAK activation and mitochondrial apoptosis. Science 2003;301:513–7.
Ciccocioppo R, Economidou D, Cippitelli A, Cucculelli M, Ubaldi M, Soverchia L, Lourdusamy A, Massi M. Genetically selected Marchigian Sardinian alcohol-preferring (msP) rats: an animal model to study the neurobiology of alcoholism. Addict Biol 2006;11:339–55.
Cozzoli DK, Goulding SP, Zhang PW, Xiao B, Hu JH, Ary AW, Obara I, Rahn A, Abou-Ziab H, Tyrrel B, Marini C, Yoneyama N, Metten P, Snelling C, Dehoff MH, Crabbe JC, Finn DA, Klugmann M, Worley PF, Szumlinski KK. Binge drinking upregulates accumbens mGluR5-Homer2-PI3K signaling: functional implications for alcoholism. J Neurosci 2009;29:8655–68.
Curtin LI, Grakowsky JA, Suarez M, Thompson AC, DiPirro JM, Martin LB, et al. Evaluation of buprenorphine in a postoperative pain model in rats. Comp Med 2009;59:60–71.
Djuricic B, Olson SR, Assaf HM, Whittingham TS, Lust WD, Drewes LR. Formation of free choline in brain tissue during in vitro energy deprivation. J Cereb Blood Flow Metab 1991;11:308–13.
Durazzo TC, Pathak V, Gazdzinski S, Mon A, Meyerhoff DJ. Metabolite levels in the brain reward pathway discriminate those who remain abstinent from those who resume hazardous alcohol consumption after treatment for alcohol dependence. J Stud Alcohol Drugs 2010;71:278–89.
Edenberg HJ, Strother WN, McClintick JN, Tian H, Stephens M, Jerome RE, Lumeng L, Li TK, McBride WJ. Gene expression in the hippocampus of inbred alcohol-preferring and -nonpreferring rats. Genes Brain Behav 2005;4:20–30.
Estruch R, Nicolas JM, Salamero M, Aragon C, Sacanella E, Fernandez-Sola J, et al. Atrophy of the corpus callosum in chronic alcoholism. J Neurol Sci 1997;146: 145–51.
Etheridge N, Lewohl JM, Mayfield RD, Harris RA, Dodd PR. Synaptic proteome changes in the superior frontal gyrus and occipital cortex of the alcoholic brain. Proteomics Clin Appl 2009;3:730–42.
Eun SY, Woo IS, Jang HS, Jin H, Kim MY, Kim HJ, Lee JH, Chang KC, Kim JH, Seo HG. Identification of cytochrome c oxidase subunit 6A1 as a suppressor of Bax-induced cell death by yeast-based functional screening. Biochem Biophys Res Comm 2008;373:58–63.
Filipek A, Schneider G, Mietelska A, Figiel I, Niewiadomska G. Age-dependent changes in neuronal distribution of CacyBP/SIP: comparison to tubulin and the tau protein. J Neural Transm 2008;115:1257–64.
Flatscher-Bader T, van der Brug M, Hwang JW, Gochee PA, Matsumoto I, Niwa S, Wilce PA. Alcohol-responsive genes in the frontal cortex and nucleus accumbens of human alcoholics. J Neurochem 2005;93:359–70.
Fujishiro Y, Kishi H, Matsuda T, Fuse H, Muraguchi A. Lactate dehydrogenase A-dependent surface expression of immature thymocyte antigen-1: an implication for a novel trafficking function of lactate dehydrogenase-A during T cell development. Eur J Immunol 2000;30:516–24.
Garbi N, Tanaka S, Momburg F, Hammerling GJ. Impaired assembly of the major histocompatibility complex class I peptide-loading complex in mice deficient in the oxidoreductase ERp57. Nat Immunol 2006;7:93–102.
Goez H, Sira LB, Jossiphov J, Borochowitz Z, Durling H, Laing NG, Nevo Y. Predominantly upper limb weakness, enlarged cisterna magna, and borderline intelligence in a child with de novo mutation of the skeletal muscle alpha-actin gene. J Child Neurol 2005;20:236–9.
Griffin JL, Mann CJ, Scott J, Shoulders CC, Nicholson JK. Choline containing metabolites during cell transfection: an insight into magnetic resonance spectroscopy detectable changes. FEBS Lett 2001;509:263–6.
Hargreaves GA, Quinn H, Kashem MA, Matsumoto I, McGregor IS. Proteomic analysis demonstrates adolescent vulnerability to lasting hippocampal changes following chronic alcohol consumption. Alcohol Clin Exp Res 2009;33:86–94.
Harper C. The neuropathology of alcohol-related brain damage. Alcohol Alcohol 2009;44:136–40.
Harper CG, Kril JJ. Corpus callosal thickness in alcoholics. Br J Addict 1988;83:577–80.
He X, Sullivan EV, Stankovic RK, Harper CG, Pfefferbaum A. Interaction of thiamine deficiency and voluntary alcohol consumption disrupts rat corpus callosum ultrastructure. Neuropsychopharmacology 2007;32:2207–16.
Hill SY, Shen S, Zezza N, Hoffman EK, Perlin M, Allan W. A genome wide search for alcoholism susceptibility genes. Am J Med Genet B Neuropsychiatr Genet 2004;128B:102–13.
Hitzemann R, Reed C, Malmanger B, Lawler M, Hitzemann B, Cunningham B, McWeeney S, Belknap J, Harrington C, Buck K, Phillips T, Crabbe J. On the integration of alcohol-related quantitative trait loci and gene expression analyses. Alcohol Clin Exp Res 2004;28:1437–48.
Hoffman P, Tabakoff B. Gene expression in animals with different acute responses to ethanol. Addict Biol 2005;10:63–9.
Ishigure K, Shimomura Y, Murakami T, Kaneko T, Takeda S, Inoue S, et al. Human liver disease decreases methacrylyl-CoA hydratase and beta-hydroxyisobutyryl-CoA hydrolase activities in valine catabolism. Clin Chim Acta 2001;312:115–21.
Iwamoto K, Bundo M, Yamamoto M, Ozawa H, Saito T, Kato T. Decreased expression of NEFH and PCP4/PEP19 in the prefrontal cortex of alcoholics. Neurosci Res 2004;49: 379–85.
Kalivas PW, O'Brien C. Drug addiction as a pathology of staged neuroplasticity. Neuropsychopharmacology 2008;33:166–80.
Kang BH, Altieri DC. Regulation of survivin stability by the aryl hydrocarbon receptor-interacting protein. J Biol Chem 2006;281:24721–7.
Kashem MA, Harper C, Matsumoto I. Differential protein expression in the corpus callosum (genu) of human alcoholics. Neurochem Int 2008;53:1–11.
Kashem MA, James G, Harper C, Wilce P, Matsumoto I. Differential protein expression in the corpus callosum (splenium) of human alcoholics: a proteomics study. Neurochem Int 2007;50:450–9.
Keller A, Nesvizhskii AI, Kolker E, Aebersold R. Empirical statistical model to estimate the accuracy of peptide identifications made by MS/MS and database search. Anal Chem 2002;74:5383–92.
Kerns RT, Ravindranathan A, Hassan S, Cage MP, York T, Sikela JM, Williams RW, Miles MF. Ethanol-responsive brain region expression networks: implications for behavioral responses to acute ethanol in DBA/2J versus C57BL/6J mice. J Neurosci 2005;25:2255–66.
Kimpel MW, Strother WN, McClintick JN, Carr LG, Liang T, Edenberg HJ, McBride WJ. Functional gene expression differences between inbred alcohol-preferring and -non-preferring rats in five brain regions. Alcohol 2007;41:95–132.
Koob GF, Volkow ND. Neurocircuitry of addiction. Neuropsychopharmacology 2010;35: 217–38.
Lewohl JM, Wang L, Miles MF, Zhang L, Dodd PR, Harris RA. Gene expression in human alcoholism: microarray analysis of frontal cortex. Alcohol Clin Exp Res 2000;24: 1873–82.
Lewohl JM, Van Dyk DD, Craft GE, Innes DJ, Mayfield RD, Cobon G, et al. The application of proteomics to the human alcoholic brain. Ann NY Acad Sci 2004;1025:14–26.
Liu J, Lewohl JM, Harris RA, Iyer VR, Dodd PR, Randall PK, Mayfield RD. Patterns of gene expression in the frontal cortex discriminate alcoholic from nonalcoholic individuals. Neuropsychopharmacology 2006;31:1574–82.
Mader I, Rauer S, Gall P, Klose U. ^{1}H MR spectroscopy of inflammation, infection and ischemia of the brain. Eur J Radiol 2008;67:250–7.

Mailliard WS, Diamond I. Recent advances in the neurobiology of alcoholism: the role of adenosine. Pharmacol Ther 2004;101:39–46.
Maldve RE, Zhang TA, Ferrani-Kile K, Schreiber SS, Lippmann MJ, Snyder GL, et al. DARPP-32 and regulation of the ethanol sensitivity of NMDA receptors in the nucleus accumbens. Nat Neurosci 2002;5:641–8.
Mann RE, Smart RG, Govoni R. The epidemiology of alcoholic liver disease. Alcohol Res Health 2003;27:209–19.
Martel G, Nishi A, Shumyatsky GP. Stathmin reveals dissociable roles of the basolateral amygdala in parental and social behaviors. Proc Natl Acad Sci USA 2008;105: 14620–5.
Masuo Y, Imai T, Shibato J, Hirano M, Jones OA, Maguire ML, et al. Omic analyses unravels global molecular changes in the brain and liver of a rat model for chronic Sake (Japanese alcoholic beverage) intake. Electrophoresis 2009;30:1259–75.
Matsuda-Matsumoto H, Iwazaki T, Kashem MA, Harper C, Matsumoto I. Differential protein expression profiles in the hippocampus of human alcoholics. Neurochem Int 2007;51:370–6.
Matsumoto I. Proteomics approach in the study of the pathophysiology of alcohol-related brain damage. Alcohol Alcohol 2009;44:171–6.
Mayfield RD, Lewohl JM, Dodd PR, Herlihy A, Liu J, Harris RA. Patterns of gene expression are altered in the frontal and motor cortices of human alcoholics. J Neurochem 2002;81:802–13.
McBride WJ, Schultz JA, Kimpel MW, McClintick JN, Wang M, You J, et al. Differential effects of ethanol in the nucleus accumbens shell of alcohol-preferring (P), alcohol-non-preferring (NP) and Wistar rats: a proteomics study. Pharmacol Biochem Behav 2009;92:304–13.
McBride WJ, Kimpel MW, Schultz JA, McClintick JN, Edenberg HJ, Bell RL. Changes in gene expression in regions of the extended amygdala of alcohol-preferring rats after binge-like alcohol drinking. Alcohol 2010;44:171–83.
Mulligan MK, Ponomarev I, Hitzemann RJ, Belknap JK, Tabakoff B, Harris RA, Crabbe JC, Blednov YA, Grahame NJ, Phillips TJ, Finn DA, Hoffman PL, Iyer VR, Koob GF, Bergeson SE. Toward understanding the genetics of alcohol drinking through transcriptome meta-analysis. Proc Natl Acad Sci USA 2006;103:6368–73.
Nesvizhskii AI, Aebersold R. Analysis, statistical validation and dissemination of large-scale proteomics datasets generated by tandem MS. Drug Discov Today 2004;9: 173–81.
Pentney RJ, Dlugos CA. Cerebellar Purkinje neurons with altered terminal dendritic segments are present in all lobules of the cerebellar vermis of ageing, ethanol-treated F344 rats. Alcohol Alcohol 2000;35:35–43.
Pfefferbaum A, Adalsteinsson E, Sullivan EV. Dysmorphology and microstructural degradation of the corpus callosum: interaction of age and alcoholism. Neurobiol Aging 2006;27:994–1009.
Pfefferbaum A, Lim KO, Desmond JE, Sullivan EV. Thinning of the corpus callosum in older alcoholic men: a magnetic resonance imaging study. Alcohol Clin Exp Res 1996;20:752–7.
Pfefferbaum A, Rosenbloom M, Rohlfing T, Sullivan EV. Degradation of association and projection white matter systems in alcoholism detected with quantitative fiber tracking. Biol Psychol 2009;65:680–90.
Pfefferbaum A, Rosenbloom MJ, Serventi KL, Sullivan EV. Brain volumes, RBC status, and hepatic function in alcoholics after 1 and 4 weeks of sobriety: predictors of outcome. Am J Psychiatry 2004;161:1190–6.
Pfefferbaum A, Zahr NM, Mayer D, Vinco S, Orduna J, Rohlfing T, et al. Ventricular expansion in wild-type Wistar rats after alcohol exposure by vapor chamber. Alcohol Clin Exp Res 2008;32:1459–67.
Pitkin SR, Savage LM. Aging potentiates the acute and chronic neurological symptoms of pyrithiamine-induced thiamine deficiency in the rodent. Behav Brain Res 2001;119:167–77.
Prescott CA, Sullivan PF, Kuo PH, Webb BT, Vittum J, Patterson DG, Thiselton DL, Myers JM, Devitt M, Halberstadt LJ, Robinson VP, Neale MC, van den Oord EJ, Walsh D, Riley BP, Kendler KS. Genomewide linkage study in the Irish affected sib pair study of alcohol dependence: evidence for a susceptibility region for symptoms of alcohol dependence on chromosome 4. Mol Psychiatry 2006;11:603–11.
Rahman-Roblick R, Roblick UJ, Hellman U, Conrotto P, Liu T, Becker S, Hirschberg D, Jornvall H, Auer G, Wiman KG. p53 targets identified by protein expression profiling. Proc Natl Acad Sci USA 2007;104:5401–6.
Roberto M, Nelson TE, Ur CL, Brunelli M, Sanna PP, Gruol DL. The transient depression of hippocampal CA1 LTP induced by chronic intermittent ethanol exposure is associated with an inhibition of the MAP kinase pathway. Eur J Neurosci 2003;17:1646–54.
Roberts AJ, Heyser CJ, Cole M, Griffin P, Koob GF. Excessive ethanol drinking following a history of dependence: animal model of allostasis. Neuropsychopharmacology 2000;22:581–94.
Rodd ZA, Kimpel MW, Edenberg HJ, Bell RL, Strother WN, McClintick JN, Carr LG, Liang T, McBride WJ. Differential gene expression in the nucleus accumbens with ethanol self-administration in inbred alcohol-preferring rats. Pharmacol Biochem Behav 2008;89:481–98.
Saba L, Bhave SV, Grahame N, Bice P, Lapadat R, Belknap J, Hoffman PL, Tabakoff B. Candidate genes and their regulatory elements: alcohol preference and tolerance. Mamm Genome 2006;17:669–88.
Sabell I, Morata P, Quesada J, Morell M. Effect of thyroid hormones on the glycolytic enzyme activity in brain areas of the rat. Enzyme 1985;34:27–32.
Saigoh K, Wang YL, Suh JG, Yamanishi T, Sakai Y, Kiyosawa H, Harada T, Ichihara N, Wakana S, Kikuchi T, Wada K. Intragenic deletion in the gene encoding ubiquitin carboxy-terminal hydrolase in gad mice. Nat Genet 1999;23:47–51.
Saito M, Szakall I, Toth R, Kovacs KM, Oros M, Prasad VV, Blumenberg M, Vadasz C. Mouse striatal transcriptome analysis: effects of oral self-administration of alcohol. Alcohol 2004;32:223–41.
Sokolov BP, Jiang L, Trivedi NS, Aston C. Transcription profiling reveals mitochondrial, ubiquitin and signaling systems abnormalities in postmortem brains from subjects with a history of alcohol abuse or dependence. J Neurosci Res 2003;72:756–67.
Sommer W, Hyytia P, Kiianmaa K. The alcohol-preferring AA and alcohol-avoiding ANA rats: neurobiology of the regulation of alcohol drinking. Addict Biol 2006;11:289–309.
Sullivan EV, Harding AJ, Pentney R, Dlugos C, Martin PR, Parks MH, et al. Disruption of frontocerebellar circuitry and function in alcoholism. Alcohol Clin Exp Res 2003;27: 301–9.
Sullivan EV, Rohlfing T, Pfefferbaum A. Pontocerebellar volume deficits and ataxia in alcoholic men and women: no evidence for “telescoping”. Psychopharmacology 2010;208:279–90.
Tabakoff B. Neurotransmitter function and alcoholism. Alcohol Clin Exp Res 1979;3: 351–2.
Tabakoff B, Bhave SV, Hoffman PL. Selective breeding, quantitative trait locus analysis, and gene arrays identify candidate genes for complex drug-related behaviors. J Neurosci 2003;23:4491–8.
Tabakoff B, Saba L, Kechris K, Hu W, Bhave SV, Finn DA, Grahame NJ, Hoffman PL. The genomic determinants of alcohol preference in mice. Mamm Genome 2008;19: 352–65.
Tabakoff B, Saba L, Printz M, Flodman P, Hodgkinson C, Goldman D, Koob G, Richardson HN, Kechris K, Bell RL, Hubner N, Heinig M, Pravenec M, Mangion J, Legault L, Dongier M, Conigrave KM, Whitfield JB, Saunders J, Grant B, Hoffman PL. Genetical genomic determinants of alcohol consumption in rats and humans. BMC Biol 2009;7:70.
Taniguchi K, Nonami T, Nakao A, Harada A, Kurokawa T, Sugiyama S, et al. The valine catabolic pathway in human liver: effect of cirrhosis on enzyme activities. Hepatology 1996;24:1395–8.
Tarnowska-Dziduszko E, Bertrand E, Szpak G. Morphological changes in the corpus callosum in chronic alcoholism. Folia Neuropathol 1995;33:25–9.
Thibault C, Lai C, Wilke N, Duong B, Olive MF, Rahman S, Dong H, Hodge CW, Lockhart DJ, Miles MF. Expression profiling of neural cells reveals specific patterns of ethanol-responsive gene expression. Mol Pharmacol 2000;58:1593–600.
Treadwell JA, Singh SM. Microarray analysis of mouse brain gene expression following acute ethanol treatment. Neurochem Res 2004;29:357–69.
Volkow ND, Hitzemann R, Wolf AP, Logan J, Fowler JS, Christman D, et al. Acute effects of ethanol on regional brain glucose metabolism and transport. Psychol Res 1990;35:39–48.
Wang J, Gutala R, Sun D, Ma JZ, Sheela RC, Ticku MK, Li MD. Regulation of platelet-derived growth factor signaling pathway by ethanol, nicotine, or both in mouse cortical neurons. Alcohol Clin Exp Res 2007;31:357–75.
Witzmann FA. Preparation of mammalian tissue samples for two-dimensional electrophoresis. In: Walker JM, editor. The proteomics protocols handbook. Totowa: The Humana Press; 2005. p. 31–5.
Witzmann FA, Li J, Strother WN, McBride WJ, Hunter L, Crabb DW, et al. Innate differences in protein expression in the nucleus accumbens and hippocampus of inbred alcohol-preferring and -nonpreferring rats. Proteomics 2003;3:1335–44.
Xu Y, Ehringer M, Yang F, Sikela JM. Comparison of global brain gene expression profiles between inbred long-sleep and inbred short-sleep mice by high-density gene array hybridization. Alcohol Clin Exp Res 2001;25:810–8.
Zahr NM, Gu M, Mayer D, Spielman D, Sullivan EV, Pfefferbaum A. Glutamate and glutamine changes induced by ethanol treatment in the rat brain detectable with CT-PRESS at 3T. Stockholm, Sweden: International Society for Magnetic Resonance Imaging; 2010a.
Zahr NM, Mayer D, Rohlfing T, Hasak M, Hsu O, Vinco S, et al. Brain injury and recovery following binge ethanol: evidence from in vivo magnetic resonance spectroscopy. Biol Psychology 2010b;67:846–54.
Zahr NM, Mayer D, Vinco S, Orduna J, Luong R, Sullivan EV, et al. In vivo evidence for alcohol-induced neurochemical changes in rat brain without protracted withdrawal, pronounced thiamine deficiency, or severe liver damage. Neuropsychopharmacology 2009;34:1427–42.
Zahr NM, Pitel AL, Chanraud S, Sullivan EV. Contributions of Studies on Alcohol Use Disorders to Understanding Cerebellar Function. Neuropsychol Rev 2010:280–9 (Epub).
Zeisel SH. Choline phospholipids: signal transduction and carcinogenesis. FASEB J 1993;7:551–7.